Journal of Solid State Chemistry **148,** 26–40 (1999)
Article ID jssc.1999.8330, available online at http://www.idealibrary.com on IDEAL®

Comparative Study of Some Layered Hydroxide Salts Containing Exchangeable Interlayer Anions

Steven P. Newman and William Jones[1]

Department of Chemistry, University of Cambridge, Lensfield Road, Cambridge, CB2 1EW, United Kingdom

Received January 8, 1999; in revised form April 2, 1999; accepted April 12, 1999

Anion-exchange reactions of layered Zn, Cu, Ni, or La hydroxide nitrates with the organic anions acetate, terephthalate, and benzoate are compared. Powder X-ray diffraction (PXRD), Fourier-transform infrared spectroscopy (FTIR), and thermogravimetry combined with mass spectrometry (TG–MS) are used to characterize the materials. Exchange of the interlayer nitrate anions for these organic anions is generally possible, although no exchange is observed for the parent nickel hydroxide material. The organo derivatives obtained may be considered inorganic–organic hybrids, consisting of alternating hydroxide and A^- layers, where A is the incorporated organic anion. The materials are structurally similar to the layered double hydroxide family of materials, which also exhibit an anion-exchange capacity.

1. INTRODUCTION

Layered materials that are able to intercalate neutral guest molecules or to exchange interlayer inorganic or organic anions attract considerable attention. An attractive feature of such layered hosts is that they may serve as templates for the creation of intercalated supramolecular arrays. Although a variety of layered materials possessing cation-exchange properties are known (such as cationic clays or metal phosphates and phosphonates), layered materials that possess anion-exchange properties are comparatively rare (1).

The most studied anion-exchangeable layered materials are the layered double hydroxide (LDH) family of materials, which consist of positively charged hydroxide layers and interlayer, charge-balancing anions. The most important group of LDHs may be represented by the formula $[M^{2+}_{1-x}M^{3+}_x(OH)_2][(x/n)A^{n-}\cdot mH_2O]$, where M^{2+} and M^{3+} are divalent and trivalent cations, respectively; x is equal to the ratio $M^{3+}/(M^{2+}+M^{3+})$, and A is an anion of valence n (2, 3). The structure of this group of LDHs is most clearly described by considering the brucite-like structure, $M(OH)_2$, which consists of M^{2+} cations coordinated octahedrally by hydroxide ions, with the octahedral units sharing edges to form infinite charge-neutral layers. In such brucite-based LDHs, isomorphous replacement of a fraction of the divalent cations with a trivalent cation occurs and generates a positive charge on the layers that necessitates the presence of interlayer, (exchangeable) anions. The anion-exchange capacity depends on the M^{2+}/M^{3+} ratio of the LDH.

LDHs may also be described on the basis of the gibbsite, $Al(OH)_3$, structure where the positive layer charge arises from the incorporation of a monovalent cation into vacancies within the sheets of $Al(OH)_6$ octahedra. An example is $[LiAl_2(OH)_6]^+A^-\cdot mH_2O$ (4).

The anion-exchange properties of LDHs have been studied extensively and are well known (5–7). In general there is no significant restriction to the nature of the anion that can occupy the interlayer of a LDH and exchange of the interlayer anions is possible for both the brucite- and gibbsite-based materials. One particular subgroup of LDHs is that in which the charge-balancing anion is organic (organo-LDHs) (8). In a series of recent publications, for example, the properties of LDHs containing terephthalate and benzoate were compared from an experimental and a molecular modeling viewpoint (9–14). Interesting interstratified phases were monitored and the influence of layer charge and degree of hydration on anion orientation was reported. Such organo-LDHs have also been shown to be effective intermediates during the incorporation of large polyoxometallate anions (15, 16). The thermal characteristics of organo-LDHs have also been reported (8). Organo-LDHs also have been shown to be effective vehicles for promoting novel photoinduced reactions (17–19).

It has recently been demonstrated that layered hydroxide (or basic) salts of certain divalent metals will also undergo anion-exchange reactions (20–27). In general, the structure of such layered hydroxide salts may be considered as an alternating sequence of modified brucite-like hydroxide layers and interlayer anions. Layered hydroxide salts are,

[1] To whom correspondence should be addressed. Fax: (01223) 336362. E-mail: wj10@cam.ac.uk.

0022-4596/99 $30.00

therefore, structurally similar to LDHs, although the origin of the anion-exchange capacity of the materials is different.

The synthesis, characterization, and anion-exchange properties of layered hydroxide salts have been much less widely studied than for LDHs. The layered hydroxide salts for which anion-exchange reactions have been reported previously may be classified into two structural types, based on the structure of either zinc or copper hydroxide nitrate with the compositions $Zn_5(OH)_8(NO_3)_2 \cdot 2H_2O$ and $Cu_2(OH)_3NO_3$ (where, in these cases, nitrate is the exchangeable anion). In particular, the anion-exchange properties of related materials in which a fraction of the Zn^{2+} or Cu^{2+} cations were isomorphously substituted for a second divalent cation have been studied (referred to as hydroxy double salts) (20, 26–28). In the present work, the synthesis and characterization of the single-metal layered hydroxide nitrates with the ideal compositions $Zn_5(OH)_8(NO_3)_2 \cdot 2H_2O$, $Cu_2(OH)_3NO_3$, $Ni_2(OH)_3(NO_3)$, and $La(OH)_2NO_3 \cdot H_2O$ are reported. Anion-exchange-type reactions of these parent hydroxide nitrates with the organic anions acetate, terephthalate, and benzoate are compared. These simple organic anions were chosen for the present study to permit straightforward comparison of the resulting organo derivatives with the corresponding organo-LDHs.

The structure of $Zn_5(OH)_8(NO_3)_2 \cdot 2H_2O$ has been determined by single crystal XRD and consists of brucite-like layers in which one-fourth of the octahedral sites are vacant (29). On either side of the vacant octahedra are located tetrahedrally coordinated Zn^{2+} cations. The tetrahedra are formed by three OH groups of the brucite-like layers (forming the base of the tetrahedron) and a water molecule. Nitrate anions are present between the hydroxide layers and are not involved in the coordination of the Zn^{2+} cations (Fig. 1a).

The structure of $Cu_2(OH)_3NO_3$ has been determined by single-crystal XRD and may be described as having brucite-like $M(OH_2)$ layers in which one-fourth of the OH^- ions are replaced by nitrate (30). The nitrate anion is located in the

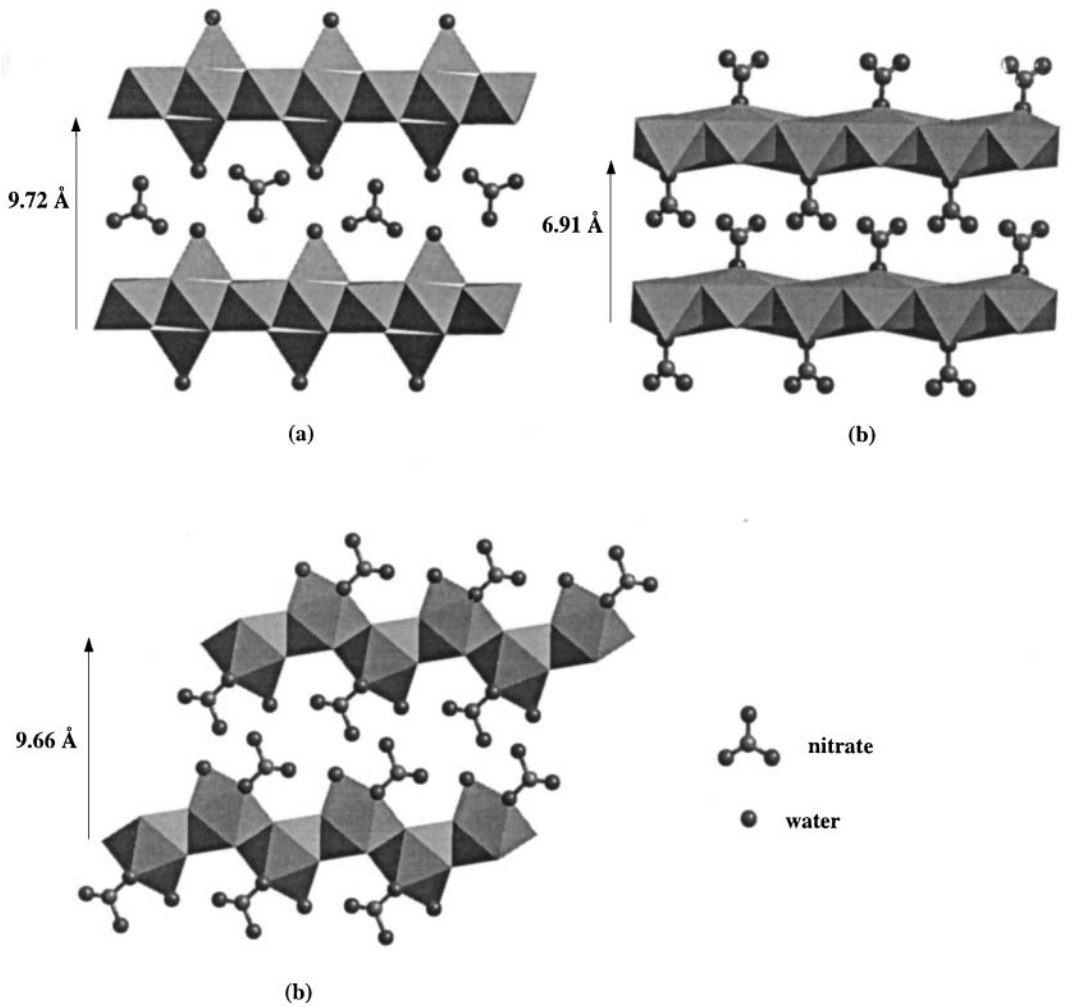

FIG. 1. Schematic representation of the structures of (a) $Zn_5(OH)_8(NO_3)_2 \cdot 2H_2O$, (b) $Cu_2(OH)_3NO_3$, and (c) $La(OH)_2NO_3 \cdot H_2O$.

interlayer and is co ordinated, through one oxygen atom, directly to the matrix Cu^{2+} cation (Fig. 1b). Although not refined, it is generally considered that $Ni_2(OH)_3NO_3$ is isomorphous with $Cu_2(OH)_3NO_3$ (31). The interlayer spacing (6.91 Å) of the nickel hydroxide nitrate is, for example, exactly the same as that for the analogous copper hydroxide nitrate.

The crystal structures of $La(OH)_2NO_3 \cdot H_2O$ and the corresponding dehydrated form, $La(OH)_2NO_3$, have been studied by Louër *et al.* (32) using the Rietveld refinement technique. Both structures consist of layers formed by polyhedra of nine coordinated lanthanum atoms, with the nitrate anions attached directly to the lanthanum atoms in an approximately perpendicular orientation with respect to the layers. In both cases the coordination polyhedron of the lanthanum atoms is a tricapped trigonal prism. In the hydrated phase, the nitrate group acts as a monodentate ligand and a water molecule is linked to one La (Fig. 1c). Removal of a water molecule from $La(OH)_2NO_3 \cdot H_2O$ leaves an empty site for coordination to the La atoms. A new tricapped trigonal prism can then be formed by a change in the coordination of the nitrate groups; i.e., one of the nonbonded nitrate oxygen atoms fills the active empty site of the coordination sphere of La and the nitrate group acts as a bidentate ligand (32).

The theoretical anion-exchange capacities (assuming complete exchange of the interlayer nitrate anions) of the Zn, Cu, Ni, and La hydroxide nitrates are 3.2, 4.2, 4,3 and 4.0 meq/g, respectively, which are similar to those generally possible for LDHs (2–5 meq/g). One aim of the present work is to study the apparent ability of these types of materials to undergo anion-exchange reactions, bearing in mind that, unlike LDHs, they do not contain heterovalent cations which generate a positive charge on the hydroxide layers. Exchange of the interlayer nitrate anions in the Zn and Cu hydroxide nitrates, with terephthalate or benzoate, is reported for the first time. Furthermore, similar anion-exchange reactions of the Ni and La hydroxide nitrates are, to our knowledge, investigated for the first time. In addition, the thermal properties of the organo derivatives are studied using combined thermogravimetry and mass spectrometry. A general comparison with corresponding organo-LDHs is made.

2. EXPERIMENTAL

There are three general approaches to the synthesis of layered hydroxide nitrate salts: pyrolysis of the hydrated metal nitrate salt (33, 34); reaction of a solid oxide with the corresponding aqueous metal nitrate salt solution (20, 24, 26, 27); and precipitation (35–38) from a metal nitrate solution with sodium hydroxide. In the present work, all the parent hydroxide nitrate compounds were prepared using the latter method. This method was adopted partly because a similar procedure (constant pH coprecipitation) is commonly used for the preparation of LDHs (39). To obtain well-crystallized and single-phase products, the conditions under which the addition is performed are important.

Zinc hydroxide nitrate with the ideal composition $Zn_5(OH)_8(NO_3)_2 \cdot 2H_2O$ was prepared by precipitation from a 3.5 M solution of $Zn(NO_3)_2 \cdot 6H_2O_{(aq)}$ with 0.75 M $NaOH_{(aq)}$. Fifty milliliters of the $NaOH_{(aq)}$ solution was added dropwise to 20 ml of the $Zn(NO_3)_2 \cdot 6H_2O_{(aq)}$ solution (giving OH/Zn = 0.5) at room temperature with vigorous stirring. The white product was immediately filtered following complete addition of the $NaOH_{(aq)}$ solution, washed with deionized water, and dried at 65°C. It was found that increasing the OH/Zn ratio, or the reaction temperature, resulted in the formation of an impurity ZnO phase, in addition to the desired product.

Copper hydroxide nitrate with the ideal composition $Cu_2(OH)_3NO_3$ was prepared by precipitation from a 3.5 M solution of $Cu(NO_3)_2 \cdot 2.5H_2O_{(aq)}$ with a 0.75 M solution of $NaOH_{(aq)}$. Fifty milliliters of the $NaOH_{(aq)}$ solution was added dropwise to 20 ml of the boiling $Cu(NO_3)_2 \cdot 2.5H_2O_{(aq)}$ solution (giving OH/Cu = 0.5) with vigorous stirring. The blue-green product was immediately filtered following addition of the $NaOH_{(aq)}$ solution, washed with deionized water and dried at 65°C. A similar procedure was used to prepare the nickel hydroxide nitrate with the ideal composition $Ni_2(OH)_3NO_3$, except that following addition of the $NaOH_{(aq)}$ solution the resulting green precipitate was hydrothermally treated at 150°C, under autogenous pressure, for 18 h. Hydrothermal treatment was required to improve the crystallinity of the product.

Lanthanum hydroxide nitrate with the ideal composition $La(OH)_2(NO_3) \cdot H_2O$ was prepared using a procedure similar to that reported by Lopez-Delgado *et al.* (40). Forty milliliters of 4 M $NaOH_{(aq)}$ was added dropwise to 20 ml of 4 M $La(NO_3)_3 \cdot 6H_2O_{(aq)}$ (OH/La = 2) with vigorous stirring at 65°C. The reaction mixture was then hydrothermally treated at 150°C, under autogenous pressure, for 18 h. The solid obtained was washed with deionized water and dried in air at room temperature.

Exchange of the interlayer nitrate anions in the Zn, Cu, Ni, and La layered hydroxide nitrates was attempted for the organic anions acetate (AC), terephthalate (TA) and benzoate (BA). Although the same general procedure was used in each case, the reaction conditions (i.e., reaction temperature and time) were varied according to the identity of the metal cation and the organic anion of interest (see Results). The general procedure was as follows: separate samples (0.2 g) of the layered hydroxide nitrates were dispersed in 50 ml of 1 N aqueous solutions of Na_nA^{n-} (A = AC, BA, or TA) at room temperature; the dispersions were stirred for a period of 24 h at room temperature, following which the products were filtered, washed with deionized water, and dried in air at 65°C.

PXRD patterns were collected in transmission mode using a STOE STADI P diffractometer. Monochromatic Cu$K\alpha_1$ ($\lambda = 1.54059$ Å) radiation was selected using a curved germanium (111) monochromator. A linear position sensitive detector with an angular range of $\Delta 2\theta = 6.5°–7.0°$, and with a step size of 1° (2θ) and counting time of 240 s per step was used to collect data in the range from 2.5° to 70.0° (2θ).

TG profiles were collected on a Polymer Laboratories TGA 1500 apparatus from room temperature to 1000°C, with a heating rate of 30°C min^{-1} in a nitrogen stream (25 ml min^{-1}). Simultaneous analysis of the evolved gases was performed via mass spectrometry using a Leda Mass Mini-Lab mass spectrometer connected to the TG via a quartz transfer line (further details of the combined TG–MS apparatus have been reported elsewhere) (41). Combined TG–MS is a useful technique for following the thermal decomposition of layered materials, for which the observed TG profiles are often complicated.

Elemental analysis of C, H, and N was performed using a CE-440 Exeter Analytical, Inc. elemental analyzer. The metal content of the products was determined via TG from the corresponding oxide residue following thermal decomposition. FTIR spectra were recorded with a Nicolet 205 FTIR spectrometer using the KBr pellet technique.

3. RESULTS AND DISCUSSION

3.1. Characterization of the Parent Hydroxide Nitrate Materials

Figure 2 compares the PXRD patterns of the Cu, Ni, Zn, or La parent hydroxide nitrate materials. All the PXRD patterns were indexed by means of the indexing program DICVOL (42); the lattice parameters and corresponding figures of merit (F_N) (43) thus obtained are recorded in Table 1. The observed lattice parameters are in good agreement with previously reported data.

For $Zn_5(OH)_8(NO_3)_2 \cdot 2H_2O$, the observed interlayer spacing is 9.72 Å, which is approximately 1 Å larger than the interlayer spacing generally observed for a LDH containing interlayer nitrate anions (5). The difference is, at least in part, due to the increased thickness of the hydroxide layers in the zinc hydroxide salt. In both LDHs containing interlayer nitrate anions and the zinc hydroxide salt, the nitrate anions adopt an approximately perpendicular orientation with respect to the hydroxide layers and are not directly coordinated to the matrix cations (Fig. 1a).

The observed interlayer spacing of 6.91 Å for $Cu_2(OH)_3NO_3$ and $Ni_2(OH)_3NO_3$ is approximately 1.5 Å smaller than the interlayer spacing generally observed for a LDH containing interlayer nitrate anions. The difference reflects the fact that in these hydroxide salts the nitrate anions directly coordinate the matrix Cu^{2+} and Ni^{2+} cations within the brucite-like layers (Fig. 1b)

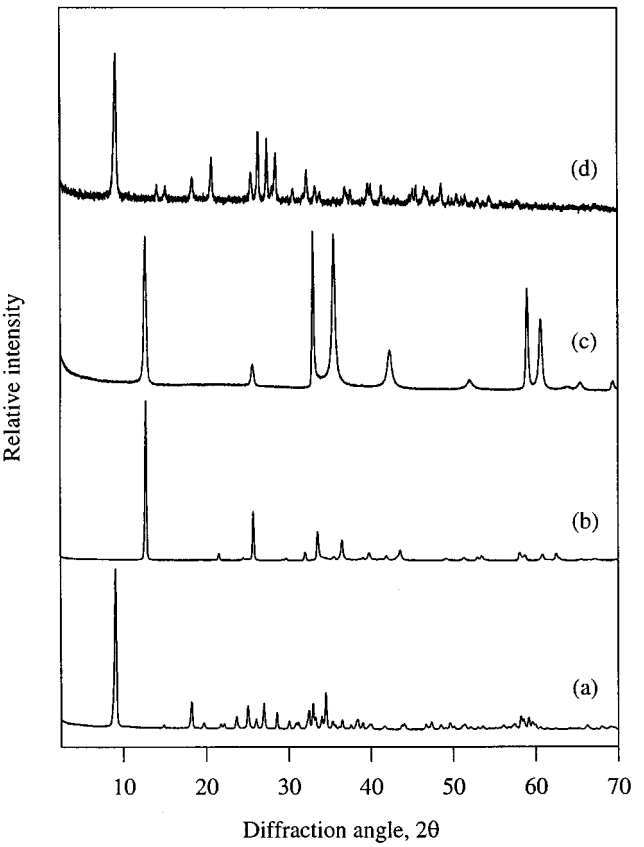

FIG. 2. PXRD patterns of (a) $Zn_5(OH)_8(NO_3)_2 \cdot 2H_2O$, (b) $Cu_2(OH)_3NO_3$, (c) $Ni_2(OH)_3NO_3$, and (d) $La(OH)_2NO_3 \cdot H_2O$.

In monoclinic $Cu_2(OH)_3NO_3$, the Cu^{2+} cations occupy two nonequivalent sites consisting of distorted 5OH + O–NO_2 or 4OH + 2(O–NO_2) octahedra (30). The Cu atoms form a pseudohexagonal net in the *ab* plane with an intermetallic Cu–Cu distance of 3.03 or 3.17 Å (30). In hexagonal $Ni_2(OH)_3NO_3$, the Ni atoms presumably form a regular hexagonal net in the *ab* plane with an intermetallic Ni–Ni distance of 3.12 Å. The hexagonal symmetry of $Ni_2(OH)_3NO_3$, therefore, indicates less distortion of the layer octahedra, compared with monoclinic $Cu_2(OH)_3NO_3$. It is well known that the Cu^{2+} (d^9) ion exhibits a strong Jahn–Teller effect, which may account for the greater distortion in the latter (38).

The observed interlayer spacing for $La(OH)_2NO_3 \cdot H_2O$ of 9.66 Å is similar to that observed for $Zn_5(OH)_8(NO_3)_2 \cdot 2H_2O$ (9.72 Å) and greater than generally observed for LDHs containing interlayer nitrate anions. The difference reflects the fact that the $La(OH)_2^+$ layers are thicker than the brucite-like, $M^{2+}(OH)_2$, layers of LDHs.

Table 2 contains the calculated compositions of the parent hydroxide nitrates, based on CHN analysis and TG data, respectively. The results are in general agreement with the expected ideal compositions, with the exception that

TABLE 1
PXRD Data for the Parent Hydroxide Nitrate Materials

Hydroxide nitrate	Observed lattice parameters	Figure of merit, $F(20)$
$Zn_5(OH)_8(NO_3)_2 \cdot 2H_2O$	C-centerd monoclinic lattice: $a = 19.473(5)$, $b = 6.239(1)$, $c = 5.519(1)$, $\beta = 93.31(2)$	$F(20) = 101.2$ (0.007, 28)
$Cu_2(OH)_3NO_3$	Monoclinic lattice: $a = 5.605(4)$, $b = 6.080(3)$, $c = 6.933(3)$, $\beta = 94.57(4)$	$F(20) = 32.9$ (0.011, 56)
$Ni_2(OH)_3NO_3$	Hexagonal lattice: $a = 3.1229(13)$, $c = 6.906(3)$	$F(16) = 53.6$ (0.018, 17)
$La(OH)_2NO_3 \cdot H_2O$	C-centerd monoclinic lattice: $a = 21.19(1)$, $b = 3.976(2)$, $c = 6.396(3)$, $\beta = 114.14(2)$	$F(20) = 53.4$ (0.011, 35)

a small number of impurity CO_3^{2-} anions are present in the products. It is well known that carbonate anions are readily incorporated and tenaciously held within the interlayer of LDHs (2, 3). The elemental analysis results indicate that the layered hydroxide salts also have a high affinity for carbonate anions.

It is useful to compare the FTIR spectra of the parent Zn, Ni, Cu, and La hydroxide nitrates (Fig. 3). In all four spectra, a strong and broad absorption due to OH stretching vibrations is observed at approximately 3500 cm^{-1}. In the region from 900 to 1600 cm^{-1}, absorption bands that may be assigned to the interlayer anion are observed (Table 3).

For $Zn_5(OH)_8(NO_3)_2 \cdot 2H_2O$, in which the interlayer nitrate is uncoordinated, the single absorption band at 1370 cm^{-1} is characteristic of the presence of an ionic nitrate group (NO_3^-, symmetry D_{3h}) (44). The FTIR spectrum is very similar to that generally observed for LDHs containing interlayer nitrate anions (45).

For $Cu_2(OH)_3NO_3$ and $Ni_2(OH)_3NO_3$, in which the nitrato group is coordinated (through one oxygen atom) to the matrix cation, the symmetry is lowered (C_{2v}) and alternative absorption bands are observed. For $Cu_2(OH)_3NO_3$, absorption bands at 1428 and 1341 cm^{-1} are assigned as the asymmetric and symmetric NO_2 stretching bands (46, 47). The absorption at 1047 cm^{-1} is assigned as the corresponding N–O stretch of the unidentate O–NO_2 group (46, 47). For $Ni_2(OH)_3NO_3$, the splitting of the asymmetric and symmetric NO_2 stretching bands is greater than for $Cu_2(OH)_3NO_3$. Furthermore, the frequency of the N–O stretching vibration is lower in the Ni hydroxide nitrate. The frequency of the N–O stretching vibration would be expected to depend on the strength of the bonding of the nitrato group to the matrix cation. Indeed, Gatehouse *et al.* found that the N–O stretching vibration of nitrato complexes shifts from 1050 cm^{-1} for ionic (uncoordinated) nitrate to 850 cm^{-1} for covalently bound, unidentate O–NO_2 (methyl nitrate) (47). This trend suggests that the nitrate group is bound more strongly to the matrix cation in $Ni_2(OH)_3NO_3$ compared with $Cu_2(OH)_3NO_3$.

For $La(OH)_2NO_3 \cdot H_2O$, in which the nitrato group is bonded through one oxygen to La, the absorption bands due to the nitrato group occur at similar frequencies as observed for $Cu_2(OH)_3NO_3$. In the spectra of the Cu, Ni,

TABLE 2
Elemental Analysis of the Zn, Ni, Cu, and La Layered Hydroxide Nitrates

Ideal formula, **Proposed formula**	Observed (%)					Calculated[a] (%)				
	C	H	N	H_2O	M	C	H	N	H_2O	M
$Zn_5(OH)_8(NO_3)_2 \cdot 2H_2O$										
$Zn_5(OH)_8(NO_3)_{1.75}(CO_3)_{0.13} \cdot 2H_2O$	0.26	1.74	3.93	4.48	51.7	0.25	1.95	3.96	5.86	52.5
$Cu_2(OH)_3NO_3$										
$Cu_2(OH)_3(NO_3)_{0.96}(CO_3)_{0.02}$	0.10	1.24	5.55	0.00	52.4	0.10	1.26	5.63	0.00	53.2
$Ni_2(OH)_3NO_3$										
$Ni_2(OH)_3(NO_3)_{0.80}(CO_3)_{0.10}$	0.57	1.36	4.37	1.20	51.4	0.54	1.34	5.00	0.00	53.5
$La(OH)_2NO_3 \cdot H_2O$										
$La(OH)_2(NO_3)_{0.74}(CO_3)_{0.13} \cdot H_2O$	0.49	1.55	4.00	7.95	55.7	0.64	1.64	4.24	7.36	56.8

[a] Calculated percentages based on the proposed formulas.

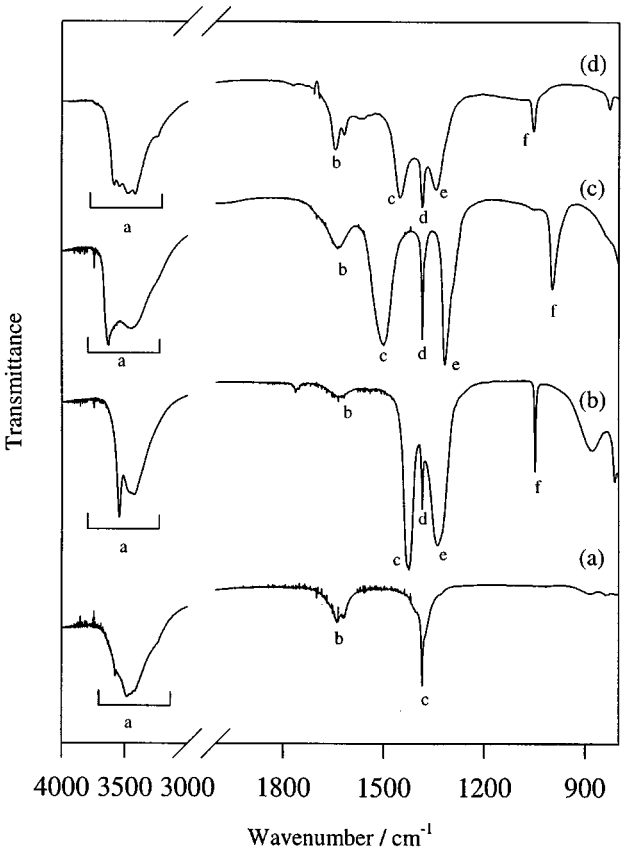

FIG. 3. FTIR spectra of (a) $Zn_5(OH)_8(NO_3)_2 \cdot 2H_2O$, (b) $Cu_2(OH)_3NO_3$, (c) $Ni_2(OH)_3NO_3$, and (d) $La(OH)_2NO_3 \cdot H_2O$. The peak assignments are summarized in Table 3.

and La hydroxide nitrates, an additional absorption band is observed at approximately 1380–1390 cm^{-1} which indicates the presence of uncoordinated nitrate. Alternatively, this absorption may be due to the presence of uncoordinated impurity carbonate anions in the materials.

TABLE 3
FTIR Data for the Parent Hydroxide Nitrates

Wavenumber (cm^{-1})				
Cu	Ni	Zn	La	Assignment
~3500(*a*)[a]	~3500(*a*)	~3500(*a*)	~3500(*a*)	H-bonding stretching vibrations of OH
1634(*b*)	1641(*b*)	1638(*b*)	1644(*b*)	H_2O bending vibration
1428(*c*)	1503(*c*)	—	1448(*c*)	O–NO_2 asymmetric stretch (C_{2v}, ν_4)
1388(*d*)	1381(*d*)	1370(*c*)	1384(*d*)	NO_3^- absorption band (D_{3h}, ν_3).
1341(*e*)	1316(*e*)	—	1332(*e*)	O–NO_2 symmetric stretch (C_{2v}, ν_1)
1047(*f*)	997(*f*)	—	1054(*f*)	N–O stretch (C_{2v}, ν_2)

[a] Letters in parentheses correspond to the peak labels used in Fig. 3.

3.2. Anion-Exchange-Type Reactions of $Zn_5(OH)_8(NO_3)_2 \cdot 2H_2O$

Figure 4 compares the PXRD patterns of the terephthalate and benzoate derivatives of $Zn_5(OH)_8(NO_3)_2 \cdot 2H_2O$. The anion-exchange reactions were performed at room temperature for 24 and 72 h for terepthalate and benzoate, respectively. The absence of reflections due to the parent material in the PXRD pattern of the terephthalate derivative indicates that exchange of nitrate for terephthalate is essentially complete after 24 h. For the benzoate derivative, however, PXRD reflections due to the unexchanged parent material remain following exchange for only 24 h; further exchange time was thus required.

Suitable solutions could not be found from DICVOL to completely index the PXRD patterns of the organo derivatives. The strongest reflections, however, may be indexed tentatively on the basis of a hexagonal lattice with unit-cell parameters $a = 6.24$ and $c = 14.5$ or 19.3 Å, for the terephthalate or benzoate derivative, respectively (20). The c parameter of the unit cell corresponds to the interlayer spacing of the organo derivative (the indexing is based on a

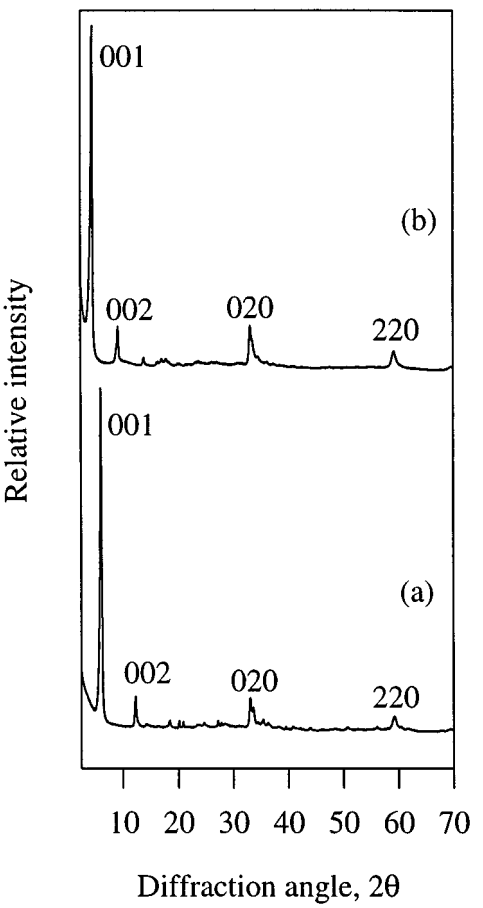

FIG. 4. PXRD patterns of the terephthalate (a) and benzoate (b) derivatives of $Zn_5(OH)_8(NO_3)_2 \cdot 2H_2O$.

single-layer repeat). The lattice parameter within the hydroxide layers of the organo derivatives ($a = 6.24$ Å) is comparable to that of the zinc hydroxide chloride with composition $Zn_5(OH)_8Cl_2 \cdot H_2O$ ($a = 6.34$, $c = 23.64$ Å), the structure of which has been described by Nowacki and Silverman in the rhombohedral space group $R\bar{3}m$ (three-layer repeat) (48, 49). The structure of $Zn_5(OH)_8Cl_2 \cdot H_2O$ is similar to that of the zinc hydroxide nitrate; the main difference is that in the nitrate form the tetrahedrally coordinated zinc atoms form a rectangular net of 6.24×5.52 Å, whereas a hexagonal net with sides 6.34 Å is formed in the chloride form. Stahlin and Oswald have studied the topotactic reaction of $Zn_5(OH)_8(NO_3)_2 \cdot 2H_2O$ with aqueous metal chloride solutions (50). It was found that anion exchange of the interlayer nitrate for chloride occurs with concomitant rearrangement of the tetrahedral zinc atoms from the rectangular to the hexagonal net. Considering the apparent hexagonal symmetry of the organo derivatives, it is possible that a similar structural rearrangement of the terahedral zinc atoms occurs on exchange of the nitrate for terephthalate or benzoate.

The observed interlayer spacing of 14.5 Å for the terephthalate derivative is similar to that generally observed for LDHs containing interlayer terephthalate anions. It is therefore proposed that the terephthalate anions adopt an approximately vertical orientation with respect to the $[Zn_5(OH)_8]^{2+}$ layers (Fig. 5a). For the benzoate derivative, the interlayer spacing of 19.3 Å is greater than that generally observed for LDHs containing interlayer benzoate anions (approximately 15–16 Å). The observed interlayer spacing nevertheless suggests a vertical bilayer arrangement of the benzoate anions between the $[Zn_5(OH)_8]^{2+}$ layers (Fig. 5b) similar to that generally proposed for the corresponding LDHs.

The product of the anion-exchange reaction with acetate was identified from the three strongest reflections (20.1°, 20.9°, and 27.2° 2θ) in the PXRD pattern (not shown) as ε-$Zn(OH)_2$ (JCPDS; File No. 12-0479 or 38-0385). No reflections that could be assigned as the basal reflections of an anion-exchange product (or of the parent hydroxide nitrate) were observed. No further characterization of the zinc hydroxide product was performed. It is interesting that anion exchange of nitrate is possible for terephthalate and benzoate but not for acetate, presumably indicating that the $[Zn_5(OH)_8]^{2+}$ hydroxide layers are not stable in aqueous solution containing the acetate anion. The initial pH of the exchange solution was 8.3, 9.5, and 9.3 for the terephthalate, benzoate, and acetate anions, respectively, suggesting that pH is not the cause of ε-$Zn(OH)_2$ formation, as might be expected. It should also be noted that Morioka *et al.* have recently prepared a zinc hydroxide acetate salt with the ideal composition $Zn_5(OH)_8(AC)_2 \cdot 2H_2O$, via direct precipitation from an aqueous zinc acetate solution (26).

The FTIR spectra of the terephthalate and benzoate derivatives of $Zn_5(OH)_8(NO_3)_2 \cdot 2H_2O$ (Fig. 6) both contain a strong and broad absorption band at approximately 3400 cm^{-1}, assigned to hydrogen–bonded OH stretching vibrations. In addition, both spectra show two strong absorption bands at approximately 1560 and 1400 cm^{-1} assigned to the asymmetric and symmetric vibrations of CO_2^-, respectively.

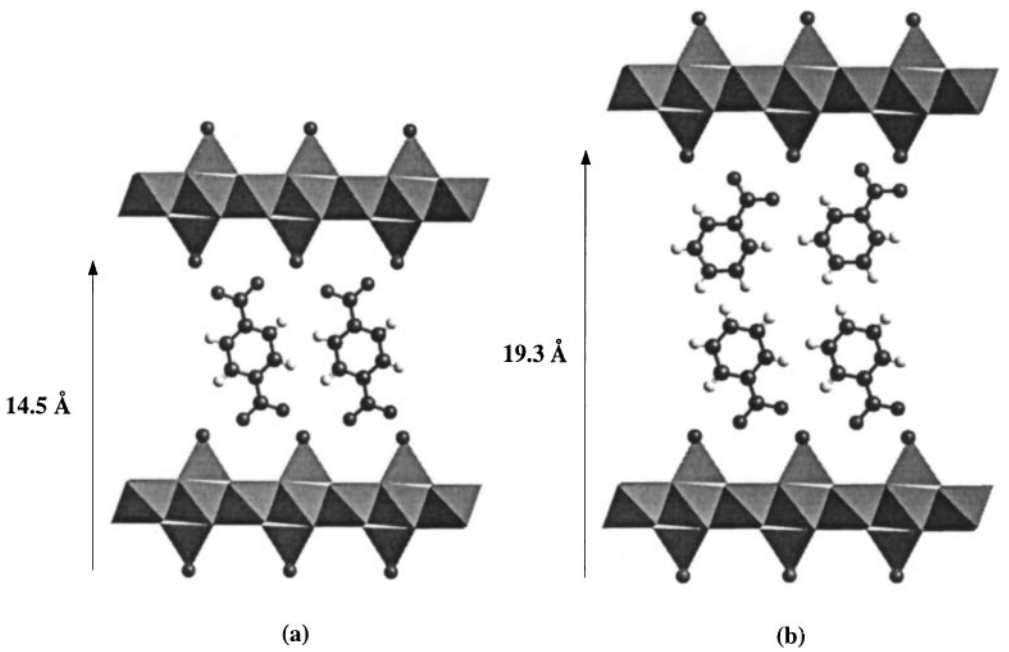

FIG. 5. Schematic illustration of the proposed structure of the (a) terephthalate and (b) benzoate derivatives of $Zn_5(OH)_8(NO_3)_2 \cdot 2H_2O$.

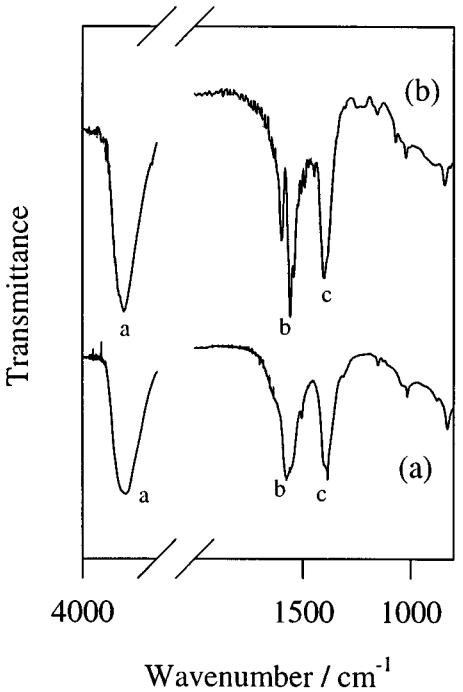

FIG. 6. FTIR spectra of the (a) terephthalate and (b) benzoate derivatives of $Zn_5(OH)_8(NO_3)_2 \cdot 2H_2O$ (a = OH stretching vibrations; b = antisymmetric and c = symmetric CO_2^- stretching vibrations).

In general, the thermal decomposition of the terephthalate and benzoate derivatives of $Zn_5(OH)_8(NO_3)_2 \cdot 2H_2O$ follows a trend similar to that observed for organo-LDHs (Fig. 7) (8). For the terephthalate derivative, the first mass loss, from room temperature to approximately 300°C, is assigned to removal of the interlayer water and dehydroxylation of the layers (detected as m/z 18, due to H_2O). The two events overlap in the TG profile, preventing calculation of an interlayer water content. A small m/z 44 signal is observed at approximately 250°C, indicating the loss of impurity carbonate anions at this temperature. The slightly lower than expected observed C content [for the proposed ideal formula $Zn_5(OH)_8TA \cdot 2H_2O$] and the absence of N also suggest that impurity carbonate is present (Table 4). Thermal decomposition of the organic occurs at approximately 500°C (detected as m/z 77, due to C_6H_5). The observed Zn content, which is in reasonable agreement with the expected value, is determined by assuming that the decomposition product at 800°C is ZnO. The TG–MS profile of the thermal decomposition of the benzoate derivative is similar to that observed for the terephthalate derivative. For the benzoate derivative the observed C content is significantly lower than the value expected for $Zn_5(OH)_8(BA)_2 \cdot 2H_2O$. The N content (from CHN analysis) and m/z 30 and 44 signals (due to NO and CO_2) at 350 and 250°C, respectively, indicate that a significant number of impurity nitrate and carbonate anions are present in the product (Table 4). The results suggest that exchange with terephthalate proceeds more efficiently than with benzoate, presumably as a consequence of the higher negative charge of the former.

3.3. *Anion-Exchange-Type Reactions of $Cu_2(OH)_3NO_3$ and $Ni_2(OH)_3NO_3$*

Figure 8 compares the PXRD patterns of the acetate, terephthalate, and benzoate derivatives of $Cu_2(OH)_3NO_3$. For the acetate derivative, the exchange reaction was performed for 24 h at room temperature [the absence of reflections due to $Cu_2(OH)_3NO_3$ in the PXRD pattern of the

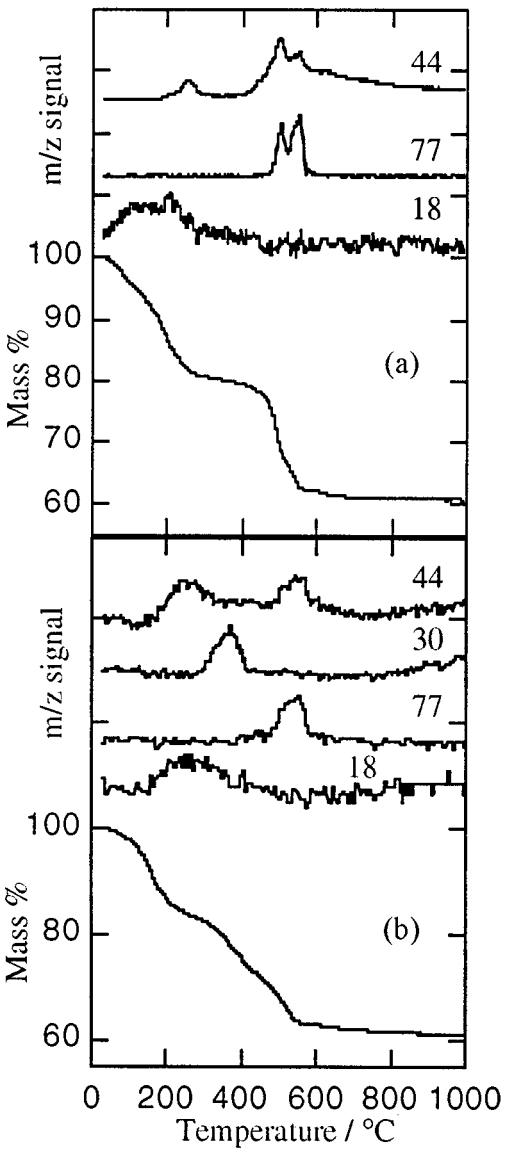

FIG. 7. TG-MS profile of the (a) terephthalate and (b) benzoate derivatives of $Zn_5(OH)_8(NO_3)_2 \cdot 2H_2O$. The m/z values correspond to the following fragments: H_2O (18), C_6H_5 (77), NO (30), CO_2 (44).

TABLE 4
Elemental Analysis Data for BA and TA Derivatives of $Zn_2(OH)_8(NO_3)_2 \cdot 2H_2O$

Ideal formula	Observed (%)					Calculated[a] (%)				
	C	H	N	H_2O	Zn	C	H	N	H_2O	Zn
$Zn_5(OH)_8TA \cdot 2H_2O$	11.52	1.96	0.0	—	48.9	14.48	2.41	0.0	5.4	49.3
$Zn_5(OH)_8(BA)_2 \cdot 2H_2O$	13.77	2.12	0.31	—	48.9	22.67	2.97	0.0	4.9	44.1

[a]Calculated percentages based on the ideal formulas.

acetate derivative suggests that exchange of nitrate for acetate is essentially complete after this time]. The PXRD pattern of the acetate derivative may be indexed on the basis of a monoclinic lattice with the refined unit-cell parameters $a = 5.606(6)$ Å, $b = 6.114(7)$ Å, $c = 9.64(1)$ Å, $\beta = 103.0(2)^\circ$, in general agreement with previously reported data [$F(20) = 21.7$ (0.033, 28)] (21, 22, 25). The lattice dimensions in the *ab* plane are similar to those of the parent hydroxide nitrate [$a = 5.605(4)$ Å, $b = 6.080(3)$ Å], although the interlayer spacing has increased from 6.91 to 9.40 Å on exchange in accordance with the larger size of the acetate anion (21, 22).

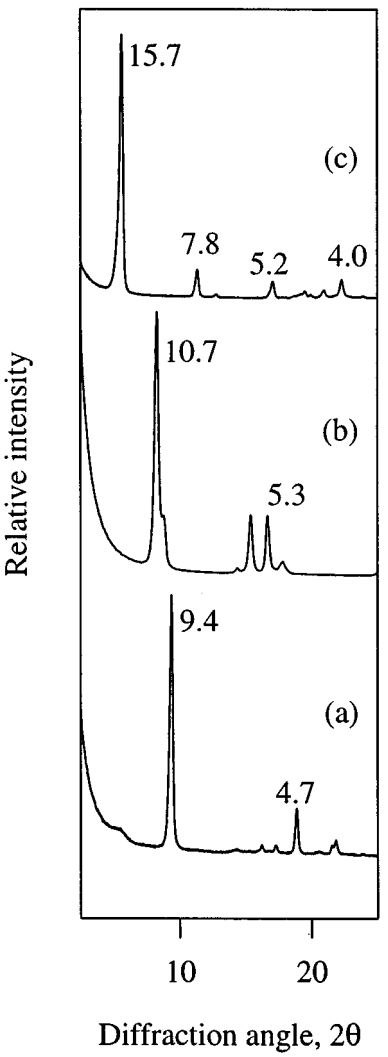

FIG. 8. PXRD patterns of the (a) acetate, (b) terephthalate, and (c) benzoate derivatives of $Cu_2(OH)_3NO_3$.

For the terephthalate derivative, the exchange reaction was also performed for 24 h at room temperature. A suitable solution could not be found to index the PXRD pattern of the terephthalate derivative thus obtained. Two reflections are tentatively indexed, however, as possible basal reflections, which correspond to an interlayer spacing of approximately 10.6 Å. If it is assumed that anion exchange of nitrate for terephthalate has occurred, and considering the bifunctional nature of terephthalate, the simplest explanation for this layer spacing is that the terephthalate anion bridges adjacent hydroxide layers in an approximately perpendicular orientation with respect to the layers. A similar interlayer arrangement is observed for LDHs containing terephthalate anions (with an interlayer spacing of approximately 14.0 Å), except that in LDHs the interlayer anion is hydrogen bonded to the hydroxide layers and not attached directly to the matrix cations. For the benzoate derivative, the exchange reaction was performed for 1 week at room temperature (unlike the acetate and terephthalate derivatives, strong reflections due to the parent material were observed following exchange for only 24 h). Again a suitable solution could not be found to index the PXRD pattern of the product, although four possible basal reflections are identified that correspond to an interlayer spacing of approximately 15.7 Å. This interlayer spacing, which is similar to that generally observed for LDHs containing interlayer benzoate anions (8), indicates that the benzoate anions form an approximately perpendicular bilayer between adjacent hydroxide layers (Fig. 9).

The blue-green parent hydroxide nitrate blackens during the exchange reactions with the organic anions, indicating the formation of CuO. No reflections due to CuO are observed in the PXRD pattern of the acetate derivative, however, suggesting that any CuO formed is amorphous,

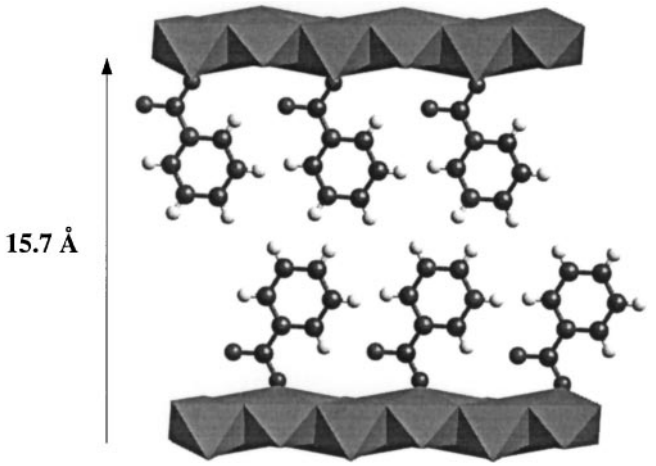

FIG. 9. Schematic illustration of the proposed structure of the benzoate derivative of $Cu_2(OH)_3NO_3$.

presumably forming on the external surfaces of the hydroxide acetate (25). For the terephthalate and benzoate derivatives, broad and weak reflections at 35.6° and 38.8° (2θ) (not shown) which may be due to the presence of CuO (JCPDS; File No. 44-0706) are observed in the PXRD patterns, possibly indicating the formation of bulk-phase CuO during the exchange process for these anions.

Anion exchange of the interlayer nitrate anions in $Ni_2(OH)_3NO_3$ was attempted for acetate, terephthalate, and benzoate at room temperature. No exchange was observed, however, after a period of 1 week for any of the organic anions (in each case the PXRD pattern following the attempted exchange was indistinguishable from the PXRD pattern of the parent hydroxide nitrate). Anion exchange for acetate was also attempted at 65°C for 72 h, although no exchange was observed. An explanation for the apparent lower reactivity of $Ni_2(OH)_3NO_3$, compared with $Cu_2(OH)_3NO_3$, is that the nitrato group is more strongly bound to the matrix cation in the former. This explanation is supported by FTIR data, which indicate that a higher degree of covalent bonding exists between the nitrato group and the metal for $Ni_2(OH)_3NO_3$ compared with $Cu_2(OH)_3NO_3$.

The FTIR spectra (not shown) of the acetate, terephthalate, and benzoate derivatives of $Cu_2(OH)_3NO_3$ all contain a strong and broad absorption due to hydrogen-bonded OH stretching vibrations at approximately 3500 cm^{-1}. In the region from 1200 to 1600 cm^{-1}, absorption bands that may be assigned to the organic interlayer anion are observed. In particular, all three spectra show two strong absorption bands at approximately 1570 and 1400 cm^{-1} assigned to the asymmetric and symmetric vibrations of CO_2^-, respectively.

The elemental composition, based on CHN analysis and TG data, of the organo derivatives of $Cu_2(OH)_3NO_3$ are recorded in Table 5. In general the observed and calculated values are in broad agreement, although each of the organo derivatives apparently contains a small fraction of unexchanged nitrate.

The TG–MS profiles of the acetate, terephthalate, and benzoate derivatives are displayed in Fig. 10. For the acetate derivative, the mass loss before 140°C indicates the presence of interlayer water. At 330°C dehydroxylation of the layers and loss of the interlayer acetate have occurred. The observed Cu content of the acetate derivative is determined by assuming that the decomposition product at 330°C is CuO (Table 5). The m/z 60 signal, observed at approximately 270°C, indicates that the organic is lost as the protonated form (CH_3CO_2H), in agreement with differential thermal analysis (DTA) data reported by Jimenez-Lopez *et al.* (an endotherm in the DTA, rather than the expected exotherm for organic decomposition was observed at 150°C) (25). A small m/z 30 signal (due to NO) is also observed at approximately 270°C, corresponding to the decomposition of impurity, unexchanged nitrate.

For the terephthalate derivative, a small mass loss (1.7%) is observed before 200°C, indicating that a small amount of water is present. Dehydroxylation of the layers begins at approximately 300°C with subsequent loss of the organic at approximately 420°C. Two m/z 44 peaks are observed; the first occurring at the same temperature as layer dehydroxylation and the second associated with decomposition of the organic. The first m/z 44 peak therefore indicates the presence of impurity carbonate anions in the material. Although CHN analysis indicates the presence of a small

TABLE 5
Elemental Analysis Data for AC, BA, and TA Derivatives of $Cu_2(OH)_3(NO_3)$

	Observed (%)					Calculated[a] (%)				
Ideal formula	C	H	N	H_2O	Cu	C	H	N	H_2O	Cu
$Cu_2(OH)_3AC \cdot H_2O$	7.80	2.40	0.11	5.9	49.2	9.41	3.14	0.0	7.06	49.8
$Cu_2(OH)_3(TA)_{0.5}$	20.48	1.44	0.11	1.7	44.0	18.45	1.92	0.0	0.0	48.9
$Cu_2(OH)_3BA$	27.03	2.25	0.27	0.0	41.3	28.07	2.67	0.0	0.0	42.5

[a] Calculated percentages based on the ideal formulas.

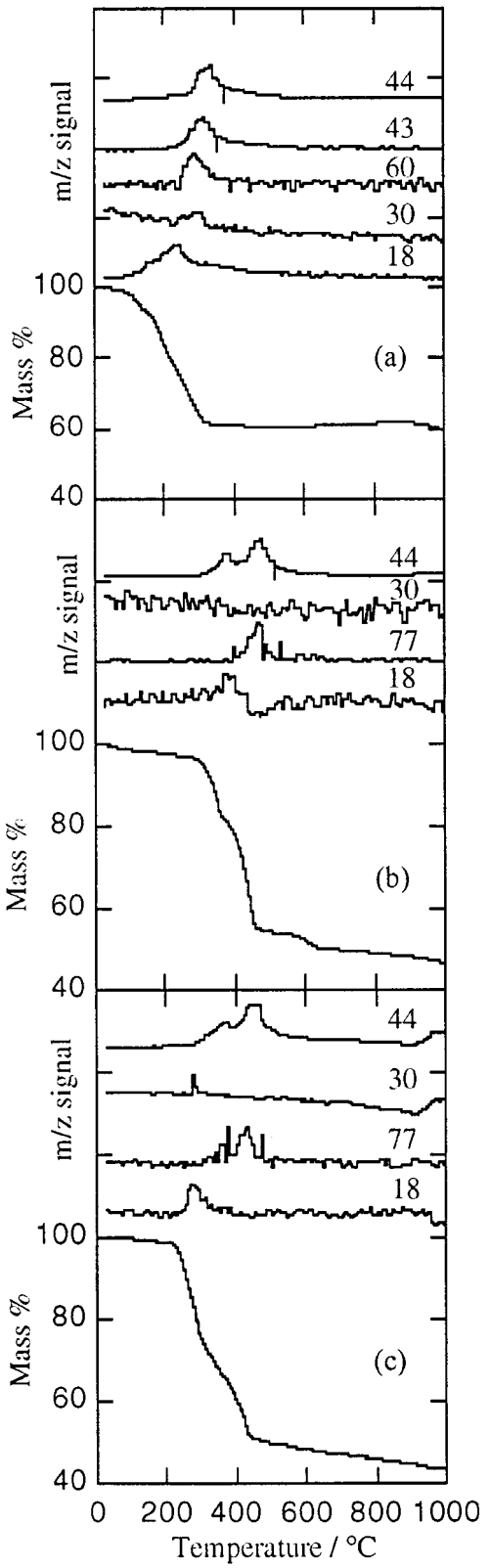

FIG. 10. TG-MS profiles of the (a) acetate, (b) terephthalate, and (c) benzoate derivatives of $Cu_2(OH)_3NO_3$. The m/z values correspond to the following fragments: H_2O (18), C_6H_5 (77), CH_3CO_2H (60), CH_3CO (43), NO (30), CO_2 (44).

number of impurity, unexchanged nitrate anions, no m/z 30 signal is detected during thermal decomposition. From approximately 450 to at least 1000°C a gradual mass loss is observed which may be due to reduction of CuO to Cu_2O and Cu^0. The thermal decomposition profile of the benzoate derivative is similar to that of the terephthalate derivative, with the onset of dehydroxylation occurring at the lower temperature of 200°C and loss of organic at approximately 400°C. The observed Cu content of the terephthalate and benzoate derivatives are determined by assuming that in each case the thermal decomposition product at approximately 450°C is CuO.

3.4. Anion-Exchange-Type reactions of $La(OH)_2NO_3 \cdot H_2O$

The elemental compositions, based on CHN analysis and TG data, of the organo derivatives of $La(OH)_2NO_3 \cdot H_2O$ are recorded in Table 6. In general, there is good agreement between observed and calculated values based on the formula $La(OH)_2(A^{n-})_{1/n} \cdot H_2O$, where A = AC, TA, or BA.

Figure 11 compares the PXRD patterns of the acetate, terephthalate, and benzoate derivatives of $La(OH)_2NO_3 \cdot H_2O$. In each case, the anion-exchange reactions were performed at 65°C for 1 week (shorter reaction times generally did not give complete exchange). No exchange was observed for any of the organic anions when the reaction was performed at room temperature. It should be noted, therefore, that the required severity of the treatment may suggest that the reactions occur via a disolution–reprecipitation mechanism, rather than direct anion exchange.

The PXRD pattern of the acetate derivative may be indexed on the basis of a triclinic lattice with the refined unit-cell parameters $a = 15.28(2)$ Å, $b = 3.929(6)$ Å, $c = 6.53(1)$ Å, $\alpha = 89.9(3)$, $\beta = 121.5(1)°$, and $\gamma = 109.2(2)°$ [$F(20) = 34.9$ (0.016, 37)]. The lattice dimensions in the bc plane are similar to those of the parent hydroxide nitrate [$b = 3.976(2)$ Å, $c = 6.396(3)$ Å, $\alpha = 90.0°$), although the interlayer spacing has increased from 9.66 to 12.0 Å ($a \sin\beta \sin\gamma$) on exchange in accordance with the larger size of the acetate anion.

The PXRD pattern of the terephthalate derivative may be indexed on the basis of a C-centred monoclinic lattice with the refined unit-cell parameters $a = 27.19(6)$ Å, $b = 3.798(7)$ Å, $c = 6.32(1)$ Å, and $\beta = 107.9(1)°$ [$F(20) = 28.1$ (0.028, 25)]. Again the lattice parameters in the bc plane are similar to those of the parent hydroxide nitrate. The interlayer spacing of the terephthalate derivative is 12.9 Å ($a/2 \sin\beta$).

A suitable solution could not be found to completely index the PXRD pattern of the benzoate derivative, possibly due to the presence of reflections from unidentified impurity phases. Three possible basal reflections, however, that correspond to an interlayer spacing of approximately 18.0 Å may be identified.

TABLE 6
Elemental Analysis Data for AC, TA, and BA Derivatives of $La(OH)_2NO_3 \cdot H_2O$

Ideal formula	Observed (%)					Calculated[a] (%)				
	C	H	N	H_2O	La	C	H	N	H_2O	La
$La(OH)_2(AC) \cdot H_2O$	9.10	2.43	0.0	7.69	56.0	9.60	2.80	0.0	7.20	55.6
$La(OH)_2(TA)_{0.5} \cdot H_2O$	17.0	2.13	0.0	6.68	51.2	17.6	2.20	0.0	6.60	50.9
$La(OH)_2(BA) \cdot H_2O$	24.19	2.47	0.0	5.80	46.3	26.93	2.88	0.0	5.77	44.5

[a] Calculated percentages based on the ideal formulas.

It is proposed that the structures of the organo derivatives are analogous to the structure of the parent $La(OH)_2NO_3 \cdot H_2O$. The structure of the acetate derivative thus consists of one oxygen of the carboxylate group of the acetate and a water molecule bonded directly to La in the hydroxide layers. The methyl group then forms a hydrophobic bilayer between the hydroxide sheets (Fig. 12). On exchange of the nitrate anions for terephthalate, the layer spacing increased to 12.9 Å. Considering the bifunctional nature of terephthalate, the simplest explanation for this interlayer spacing is that the anion bridges adjacent layers in an approximately perpendicular arrangement with respect to the hydroxide layers [similar to that proposed for the terephthalate derivative of $Cu_2(OH)_3NO_3$]. For the benzoate derivative, the interlayer spacing of 18.0 Å suggests a vertical bilayer arrangement of the benzoate anions between the hydroxide layers.

The FTIR spectra of the acetate, terephthalate, and benzoate derivatives of $La(OH)_2NO_3 \cdot H_2O$ (not shown) all contain a strong and broad absorption due to the OH stretching vibrations of the hydroxide layers and water molecules at approximately 3500 cm^{-1}. In the region from 900 to 1600 cm^{-1}, absorption bands that may be assigned to the interlayer anion are observed.

The TG profiles of the organo derivatives are similar to that reported previously for the parent hydroxide nitrate (40, 51). In each case four stages of mass loss are observed (Fig. 13, Tables 7–9). The first and second stages correspond to the removal of interlayer water and dehydroxylation of

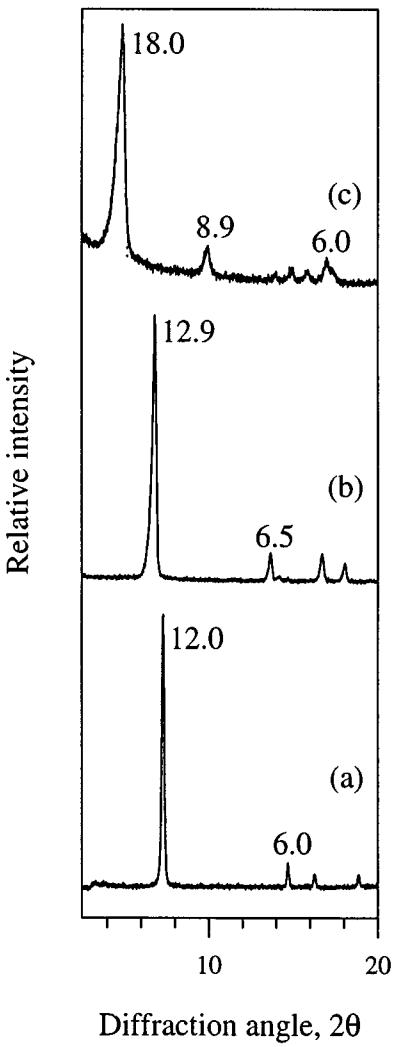

FIG. 11. PXRD patterns of the (a) acetate, (b) terephthalate, and (c) benzoate derivatives of $La(OH)_2NO_3 \cdot H_2O$.

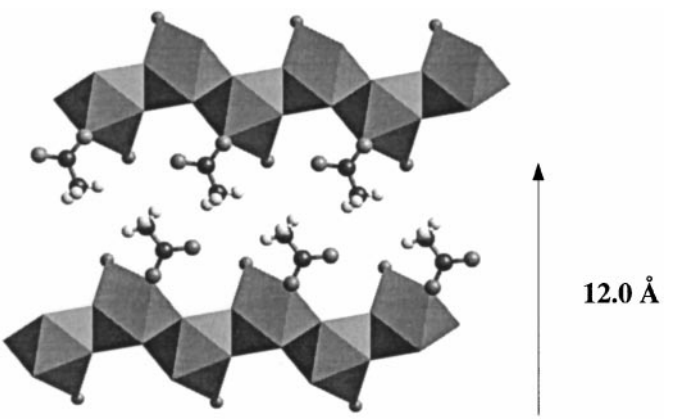

FIG. 12. Schematic illustration of the proposed structure of the acetate derivative of $La(OH)_2NO_3 \cdot H_2O$.

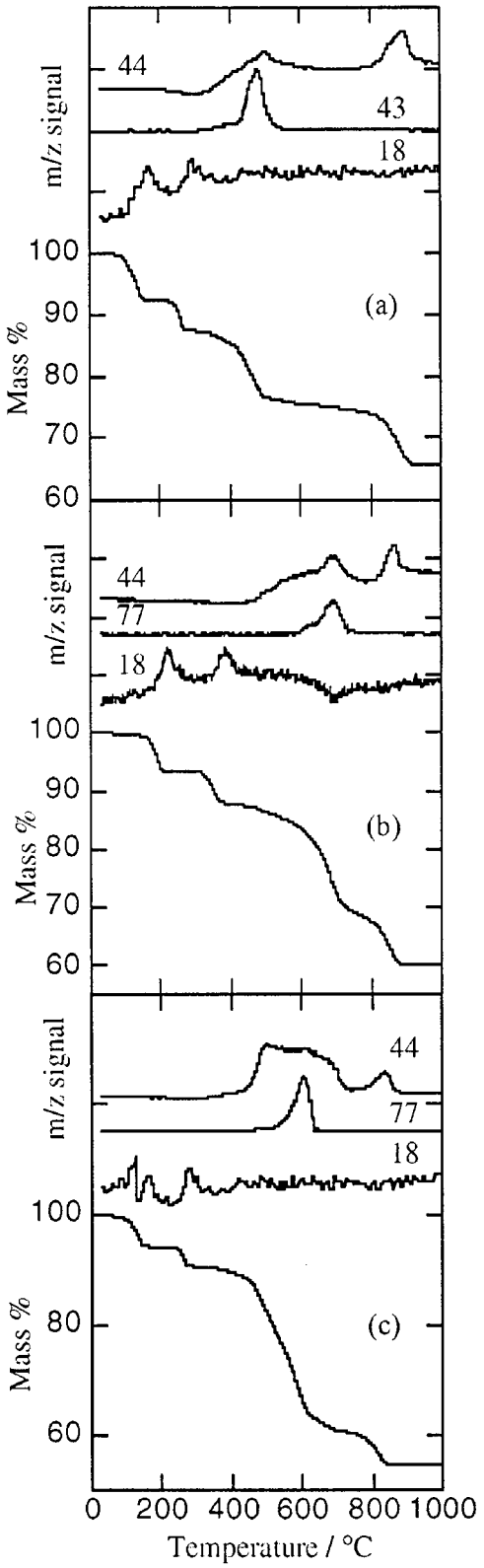

FIG. 13. TG-MS profiles of the (a) acetate, (b) terephthalate, and (c) benzoate derivatives of $La(OH)_2NO_3 \cdot H_2O$. The m/z values correspond to the following fragments: H_2O (18), C_6H_5 (77), CH_3CO (43), CO_2 (44).

TABLE 7
TG Data for the Acetate Derivative of $La(OH)_2NO_3 \cdot H_2O$

Temperature range (°C)	Mass loss (%) Obs.	Calc.	
25–200	7.7	7.20	$La(OH)_2AC \cdot H_2O \rightarrow La(OH)_2AC + H_2O$
200–300	5.0	7.20	$La(OH)_2AC \rightarrow LaOAC + H_2O$
300–660	12.2	11.62	$LaOAC \rightarrow La_2O_2CO_3$
660–1000	9.5	8.80	$La_2O_2CO_3 \rightarrow La_2O_3 + CO_2$

the hydroxide layers, respectively. The third stage corresponds to thermal decomposition of acetate (detected as m/z 43, due to C_2H_3O), terephthalate (detected as m/z 77, due to C_6H_5), or benzoate (detected as m/z 77, due to C_6H_5) at approximately 500, 700, or 600°C, respectively, with concomitant formation of $La_2O_2CO_3$. The fourth stage corresponds to the decomposition of $La_2O_2CO_3$ to La_2O_3.

4. GENERAL DISCUSSION

For $Zn_5(OH)_8(NO_3)_2 \cdot 2H_2O$, the nitrate anions, which are located between the hydroxide layers and are not involved in the coordination of the Zn cations, have been successfully exchanged with both terephthalate and benzoate. It is reasonable to conclude that the relatively weak association of the interlayer nitrate with the hydroxide layers (i.e., hydrogen-bonding interactions) facilitates such anion exchange reactions. The attempted anion exchange with acetate resulted in the formation of zinc hydroxide, suggesting that the $[Zn_5(OH)_8]^{2+}$ layers are susceptible to dissolution–reprecipitation in the presence of certain anions.

Although the nitrato group is directly coordinated to the matrix Cu cations in $Cu_2(OH)_3NO_3$, anion exchange of nitrate with acetate, terephthalate, or benzoate is possible. For the structurally similar $Ni_2(OH)_3NO_3$, no such exchange was observed for any of the anions tested under identical conditions. The different reactivity of the two

TABLE 8
TG Data for the Terephthalate Derivative of $La(OH)_2NO_3 \cdot H_2O$

Temperature range (°C)	Mass loss (%) Obs.	Calc.	
25–270	6.7	6.59	$La(OH)_2(TA)_{0.5} \cdot H_2O \rightarrow La(OH)_2(TA)_{0.5} + H_2O$
270–410	5.70	6.59	$La(OH)_2(TA)_{0.5} \rightarrow LaO(TA)_{0.5} + H_2O$
410–740	17.9	19.08	$LaO(TA)_{0.5} \rightarrow La_2O_2CO_3$
740–1000	9.6	8.06	$La_2O_2CO_3 \rightarrow La_2O_3 + CO_2$

TABLE 9
TG Data for the Benzoate Derivative of $La(OH)_2NO_3 \cdot H_2O$

Temperature range (°C)	Mass loss (%) Obs.	Calc.	
25–200	5.8	5.77	$La(OH)_2BA \cdot H_2O \rightarrow La(OH)_2BA + H_2O$
200–300	3.6	5.77	$La(OH)_2BA \rightarrow LaOBA + H_2O$
300–660	29.9	29.14	$LaOBA \rightarrow La_2O_2CO_3$
660–1000	6.27	7.05	$La_2O_2CO_3 \rightarrow La_2O_3 + CO_2$

materials is presumably related to the degree of covalent bonding of the nitrato group to the matrix cations, which has been observed to be lower in $Cu_2(OH)_3NO_3$, on the basis of FTIR data. The different M–ONO_2 bond strengths may arise from the relative distortion of the layer octahedra which is greater in the Cu material.

It should be noted that anion-exchange reactions of the cobalt hydroxide nitrate $Co_2(OH)_3NO_3$ have recently been studied by Laget and co-workers (52–54). Anion exchange of nitrate with acetate or dodecyl sulfate was achieved. In addition, Laget *et al.* recently reported the preparation and magnetic properties of a layered cobalt hydroxide salt containing the iminonitroxide benzoate radical organic anion via anion exchange of the parent $Co_2(OH)_3NO_3$ (53). The reported FTIR absorption bands of the nitrato group (1424, 1340, and 1048 cm^{-1}) in the parent cobalt material correspond almost exactly to the nitrate absorption bands observed in the present work for $Cu_2(OH)_3NO_3$, thus indicating similar bonding of the nitrato group to Cu or Co in these materials. Although not refined, the reported structure of $Co_2(OH)_3NO_3$ is monoclinic with lattice parameters ($a = 5.531$ Å, $b = 6.30$ Å, $c = 6.96$ Å, $\beta = 93.18°$) (52) comparable to those observed for $Cu_2(OH)_3NO_3$, indicating that a distortion of the constituent layer octahedra similar to that observed for the Cu material occurs in the Co material. It may therefore be inferred that distortion of the layer octahedra, with concomitant weakening of the M–ONO_2 bond, facilitates the anion-exchange reactions observed for the Co and Cu hydroxide nitrates.

The nitrato group is also directly coordinated to the matrix cation in $La(OH)_2NO_3 \cdot H_2O$. The apparent anion-exchange ability of $La(OH)_2NO_3 \cdot H_2O$ indicates, however, a predominantly electrostatic nature of the bonding of the nitrato group to La in the hydroxide layers. The high coordination number and the electropositive character of the La^{3+} cation presumably inhibit covalent bonding. The bonding of the nitrate anion to La may therefore be considered as predominantly electrostatic rather than of a directional covalent character, thus facilitating anion-exchange-type reactions. The structure may thus be represented by alternating layers of $La(OH)_2^+$ and NO_3^- approximately perpendicular to the *bc* plane.

Finally, it should be noted that direct coordination of the interlayer anion to the matrix cation in the Cu and La hydroxide salts imposes a geometrical requirement on the types of anions that may be incorporated into such materials. It is unlikely, for example, that it will be possible to incorporate bulky, highly charged anions such as the inorganic polyoxometallate anions ($[V_{10}O_{28}]^{6-}$ or $[Mo_7O_{24}]^{6-}$) commonly incorporated into LDHs (16, 55). Such polyoxometallate pillared LDHs represent a class of pillared materials for selective absorption and oxidation catalysis. In LDHs [and $Zn_5(OH)_8(NO_3)_2 \cdot 2H_2O$] the interlayer anions are located between the hydroxide layers and not involved in the coordination of the matrix metal cation and no such geometrical constraint is imposed.

5. CONCLUSIONS

The ability of certain layered hydroxide nitrates to undergo exchange of the interlayer nitrate anions with organic anions such as acetate, terephthalate, and benzoate has been demonstrated. These materials therefore complement LDHs as materials that have the characteristic potential to act as hosts for a variety of negatively charged organic or inorganic molecules. In general, the organo derivatives may be considered inorganic–organic hybrids, consisting of alternating hydroxide and A^- layers, where A^- is the incorporated organic anion.

ACKNOWLEDGMENTS

We are grateful to the EPRSC and Schlumberger Cambridge Research for support (CASE Award to S.P.N.).

REFERENCES

1. D. W. Bruce and D. O'Hare, "Inorganic Materials," Wiley, Chichester, 1997.
2. A. de Roy, C. Forano, K. El Malki, and J.-P. Besse, *in* "Anionic Clays: Trends in Pillaring Chemistry, Synthesis of Microporous Materials" (M. L. Occeli and E. R. Robson, Eds.). Van Nostrand Reinhold, New York, 1992.
3. F. Cavani, F. Trifirò, and A. Vaccari, *Catal. Today* **11,** 173 (1991).
4. A. V. Besserguenev, A. M. Fogg, R. J. Francis, S. J. Price, and D. O'Hare, *Chem. Mater.* **9,** 241 (1997).
5. S. Miyata, *Clays Clay Miner.* **31,** 305 (1983).
6. I. C. Chisem and W. Jones, *J. Mater. Chem.* **4,** 1737 (1994).
7. M. Meyn, K. Beneke, and G. Lagaly, *Inorg. Chem.* **29,** 5201 (1990).
8. S. P. Newman and W. Jones, *New J. Chem.* **22,** 105 (1998).
9. F. Kooli, I. C. Chisem, M. Vucelic, and W. Jones, *Chem. Mater.* **8,** 1969 (1996).
10. S. P. Newman, S. J. Williams, P. V. Coveney, and W. Jones, *J. Phys. Chem. B* **102,** 6710 (1998).
11. S. J. Williams, P. V. Coveney, and W. Jones, *Mol. Simul.* **21,** 183 (1999).

12. M. Aicken, I. S. Bell, P. V. Coveney, and W. Jones, *Adv. Mater.* **9,** 496 (1997).
13. I. S. Bell, F. Kooli, W. Jones, and P. V. Coveney, *Mater. Res. Soc. Symp. Proc.* **453,** 73, (1996).
14. M. Vucelic, G. D. Moggridge, and W. Jones, *J. Phys. Chem.* **99,** 8328 (1995).
15. J. Evans, M. Pillinger, and J. Zhang, *J. Chem. Soc. Dalton Trans.* **2963 (**1996).
16. M. A. Drezdzon, *Inorg. Chem.* **27,** 4628 (1988).
17. H. Tagaya, S. Sato, T. Kuwahara, J. Kadokawa, K. Masa, and K. Chiba, *J. Mater. Chem.* **4,** 1907 (1994).
18. T. Shichi, K. Takagi, and Y. Sawaki, *J. Chem. Soc. Chem. Commun.*, 2027 (1996).
19. K. Takagi, T. Shichi, H. Usami, and Y. Sawaki, *J. Am. Chem. Soc.* **115,** 4339 (1993).
20. S. Yamanaka, K. Ando, and M. Ohashi, *Mater. Res. Soc. Symp. Proc.* **371,** 131 (1995).
21. S. Yamanaka, T. Sako, K. Seki, and M. Hattori, *Solid State Ionics* **53,** 527 (1992).
22. S. Yamanaka, T. Sako, and H. Hattori, *Chem. Lett.*, 1869 (1989).
23. S. Komarneni, Q. H. Li, and R. Roy, *J. Mater. Res.* **11,** 1866 (1996).
24. H. Hayashi and M. J. Hudson, *J. Mater. Chem.* **5,** 781 (1995).
25. A. Jimenez-Lopez, E. Rodriguez-Castellon, P. Olivera-Pastor, P. Maireles-Torres, A. A. G. Tomlinson, D. J. Jones, and J. Roziere, *J. Mater. Chem.* **3,** 303 (1993).
26. H. Morioka, H. Tagaya, M. Karasu, J.-I. Kadokawa, and K. Chiba, *J. Mater. Res.* **13,** 848 (1998).
27. M. Meyn, K. Beneke, and G. Lagaly, *Inorg. Chem.* **32,** 1209 (1993).
28. H. Nishizawa and K. Yuasa, *J. Solid State Chem.* **141,** 229 (1998).
29. W. Stahlin and H. R. Oswald, *Acta Crystallogr. B* **26,** 860 (1970).
30. W. Nowacki and R. Scheidegger, *Helv. Chim. Acta*, 375 (1952).
31. M. Louër, D. Louër, and D. Grandjean, *Acta Crystallogr. B* **29,** 1696 (1973).
32. M. Louër, D. Louër, A. L. Delgado, and O. G. Martinez, *Eur. J. Solid State Inorg. Chem.* **26,** 241 (1989).
33. I. A. Kudrenko and Y. G. Dorokhov, *Russ. J. Inorg. Chem.* **18,** 17 (1973).
34. D. Louër and A. Deguibert, *J. Mater. Sci.* **20,** 3729 (1985).
35. K. Petrov, L. Markov, and P. Rachev, *React. Solids* **3,** 67 (1987).
36. K. Petrov, N. Zotov, O. Garciamartinez, P. Millan, and R. M. Rojas, *React. Solids* **7,** 359 (1989).
37. L. Markov and K. Petrov, *React. Solids* **1,** 319 (1986).
38. M. Atanasov, N. Zotov, C. Friebel, K. Petrov, and D. Reinen, *J. Solid State Chem.* **108,** 37 (1994).
39. S. P. Newman, Ph.D. thesis, University of Cambridge, 1999.
40. A. L. Delgado, C. P. Cortina, and O. G. Martinez, *Anal. Quim. B Quim. Inorg. Quim. Anal.* **80,** 189 (1984).
41. I. C. Chisem, S. D. Cosgrove, and W. Jones, *J. Therm. Anal.* **50,** 757 (1997).
42. A. Boultif and D. Louër, *J. Appl. Crystallogr.* **24,** 987 (1991).
43. G. S. Smith and R. L. Snyder, *J. Appl. Crystallogr.* **12,** 60 (1979).
44. K. Nakamoto, "Infrared and Raman Spectra of Inorganic and Coordination Compounds," Part B. Wileys, New York, 1997.
45. H. Zhao and G. F. Vance, *J. Chem. Soc. Dalton Trans.*, 1961 (1997).
46. C. C. Addison and B. M. Gatehouse, *J. Chem. Soc.*, 613 (1960).
47. B. M. Gatehouse, S. E. Livingstone, and R. S. Nyholm, *J. Chem. Soc.*, 4222 (1957).
48. W. Nowacki and J. N. Silverman, *Z. Kristallogr.* **115,** 21 (1961).
49. R. Allmann, *Z. Kristallogr.* **126,** 417 (1968).
50. W. Stahlin and H. R. Oswald, *J. Solid State Chem.* **3,** 256 (1971).
51. A.-E. Gobichon, J.-P. Auffredic, and D. Louër, *Solid State Ionics* **93,** 51 (1997).
52. V. Laget, S. Rouba, P. Rabu, C. Hornick, and M. Drillon, *J. Magn. Magn. Mater.* **154,** L7 (1996).
53. V. Laget, C. Hornick, P. Rabu, M. Drillon, P. Turek, and R. Ziessel, *Adv. Mater.* **10,** 1024 (1998).
54. M. Drillon, C. Hornick, V. Laget, P. Rabu, F. M. Romero, S. Rouba, G. Ulrich, and Z. Ziessel, *Mol. Cryst. Liq. Cryst.* **273,** 125 (1995).
55. E. Narita, P. D. Kaviratna, and T. J. Pinnavaia, *J. Chem. Soc. Chem. Commun.*, 60 (1993).